Ian Ashdown, P. Eng., LC
620 Ballantree Road
West Vancouver, B.C.
Canada V7S 1W3

Tel: (604) 922-6148
Fax: (604) 987-7621
e-mail: iashdown@cs.ubc.ca

May 12, 1999

Comparing Photometric Distributions

by

Ian Ashdown, P. Eng., LC
Department of Computer Science
University of British Columbia

1. Introduction

Illumination engineers and lighting specifiers often need to compare the photometric specifications of similar light sources. Factors such as luminaire efficiency and color temperature are easy to compare – they are scalar numbers. Photometric distributions, however, are more problematic. We must compare two-dimensional plots of intensity values in one or more planes. Worse, the comparison is inexact; we are usually interested more in the general *shape* of a distribution than in its specific values.

The criteria for comparison can vary between disciplines. The photometric distribution requirements for architectural luminaires, for example, differ greatly from those for automotive headlights. The means of measuring and reporting the photometric distributions may also vary. Still, the underlying photometric principles (and hence the problem of comparison) are essentially the same.

What we need is a technique that automatically compares "similar" photometric distributions in two and possibly three dimensions. Given a particular photometric distribution as an example (a *template*), we need to compare and quantitatively rank a set of similar distributions. For some applications, we may also need to develop heuristics to guide the comparison process.

This problem is an example of *pattern classification*. Similar problems occur in fields as diverse as cartography, satellite surveillance, biomedicine, forensics, industrial machine vision, image database retrieval, and optical character recognition. As you might expect, many techniques have been proposed to solve these problems, with thousands of papers and dozens of books having been published on the topic. Our first challenge is therefore to identify a promising technique within this body of literature.

2. Shape Analysis

Our particular problem is one of *shape analysis*, where "shape" is usually defined as the outline or silhouette of an object. In essence, shape analysis compares digitized images of three-dimensional objects based on their silhouettes (or more generally, *boundary representations*) only. Image information such as gray-scale shading and texture is simply ignored.

As noted by Loncaric (1998), shape analysis techniques are typically applied to the identification of two- and three-dimensional objects from two-dimensional images. These objects include organs and cells in biomedicine, manufactured parts in industrial machine vision, military aircraft in satellite surveillance, and characters in printed and handwritten text. Their application to photometric distributions is, well, somewhat unusual.

The approach becomes clear when we consider that each photometric distribution defines a unique three-dimensional *photometric solid* (Yamauti 1932) whose boundary is represented by the luminous intensity values in a spherical coordinate system (Figure 2). A plot of these values for a given vertical plane (Figure 1) defines the object's intersection with the plane. We can think of this intersection as a silhouette.

3. A Taxonomy of Techniques

Many shape analysis techniques have been proposed over the past three decades – Loncaric (1998) identifies over thirty of them in his survey, and he cautions readers that the list is by no means exhaustive.

This paper will consider only one of these techniques in detail. However, there are many other possible approaches to the problem of photometric distribution comparison. Given that the topic of pattern classification is foreign to illumination engineering, it is therefore useful to provide a taxonomy of existing techniques and references to a few examples in the literature.

Shape analysis techniques can be grouped into several broad classes:

- Geometric
- Transform
- Moments
- Syntactic (relational)
- Statistical

Geometric techniques model shapes as *n*-sided polygons. Their common goal is to extract a vector of real or complex numbers (a *feature set*) from the list of vertices that represents the important features of the shapes. (What is considered "important" depends of course on the problem domain.) Examples include Arkin et al. (1986), Chang et al. (1991), Goshtasby (1985), Huttenlocher et al. (1993), Lin et al. (1992), Parui and Majumder (1983), and Smith and Jain (1982).

Transform techniques model the outline as a one-dimensional function and use a Fourier or similar transform to represent it as a linear combination of orthogonal basis functions. These techniques produce arrays of real or complex coefficients that correspond to the feature sets of geometric algorithms. Representative examples include Chuang and Kuo (1996), Jacobs et al. (1995), Mallet et al. (1997), and Persoon and Fu (1977).

Moment-based techniques calculate the moments of the shapes. A *k*-dimensional nearest neighbor analysis is then usually performed to determine which of several template shapes the unknown shape most closely resembles. Representative examples include Belkasim et al. (1991) and Teague (1980).

Syntactic and relational techniques typically extract and then combine "skeletons" and other morphological features of shapes into relational models that can be analyzed as instances of formal grammars. (As you might expect, these topics are far removed from the needs of photometric distribution comparisons.) Some examples include Blum (1977), Cortelazzo et al. (1994), Pavlidis (1979), and Sze and Yang (1981).

Statistical techniques model shapes as one-dimensional signals and attempt to estimate their parameters using autoregressive modeling and other statistical techniques. Examples include Das et al. (1990), Dubois and Glanz (1986), Eom (1998), He and Kundu (1991), and Kashyap and Chellappa (1981).

There are other shape analysis techniques (e.g., Gunsel and Telkap 1998, and Neil and Curtis 1997) that fall outside of these classes, and some that combine features of two or more classes (e.g., Cohen et al. 1995 and Wang et al. 1994).

4. Comparison Metrics

Many shape analysis techniques can potentially be applied to photometric distribution comparisons, with arguments made for and against each technique. However, if we are to compare and quantitatively rank a set of similar distributions, we need a single scalar number – a *metric* – for comparison purposes.

Any metric $d(A,B)$ that measures the degree of dissimilarity between two arbitrary shapes *A* and *B* must have the following mathematical properties:

$d(A,B) \geq 0$ for all *A* and *B*

$d(A,B) = 0$ if and only if $A = B$ (identity)

$d(A,B) = d(B,A)$ for all *A* and *B* (symmetry)

$d(A,B) + d(B,C) \geq d(A,C)$ for all A, B, and C (triangle inequality)

These properties mirror our intuition about shape similarity. Identity means that we expect a shape to resemble itself and no other shape. Symmetry means that the order of comparison should not matter. The triangle inequality implies that if *A* is very similar to *B* and *B* is very similar to *C*,

then *A* and *C* are likewise similar. (This is also referred to as *stability* in the sense that a small change to a shape should engender a similarly small change in the value of the metric.)

While there have been many shape analysis techniques proposed in the literature, very few consider comparison metrics. One likely reason for this is that shapes can be characterized much more easily using multidimensional feature sets than they can be using a single number. This is useful for shape classification (the primary goal of shape analysis) using multidimensional *k*-nearest neighbor analysis, but not for ranking purposes.

Of the few metrics that have been proposed, one of the most popular has been the *Hausdorff distance metric* (e.g., Huttenlocher et al. 1993). While it may not be the best metric for comparing arbitrary polygonal curves (Godau 1991 and Alt and Godau 1992), it is well suited for simple polygonal shapes.

5. The Hausdorff Distance Metric

Following Huttenlocher et al. (1993), we can model two photometric distributions as finite point sets $A = \{a_1, \ldots, a_p\}$ and $B = \{b_1, \ldots, b_q\}$. The Hausdorff distance is then defined as:

$$H(A,B) = \max(h(A,B), h(B,A)) \tag{1}$$

where:

$$h(A,B) = \max_{a \in A} \min_{b \in B} \|a - b\| \tag{2}$$

is called the *directed* Hausdorff distance from *A* to *B*, and $\|\cdot\|$ is some norm[1] (typically the L_2, or Euclidean, norm) on the points of *A* and *B*.

The function $h(A,B)$ identifies the point $a \in A$ that is farthest (in the sense of the chosen norm) from any point $b \in B$, and measures the distance between them. Thus if $h(A,B) = d$, then each point of *A* must be within distance *d* of some point of *B*. Furthermore, there is some point of *A* that is exactly distance *d* from the nearest point of *B*. (This is the most mismatched point.)

The Hausdorff distance $H(A,B)$ is the maximum of $h(A,B)$ and $h(B,A)$, and so it measures the degree of mismatch between the two sets of points. (The directed Hausdorff distance is asymmetric in that in general, $h(A,B) \neq h(B,A)$.) If the Hausdorff distance is some value *d'*, then every point of *A* must be within distance *d'* of some point of *B*, and vice versa.

The Hausdorff distance is very sensitive to outlying points of *A* or *B*. If there is even a single point of *A* that is at some large distance *d* from the nearest point of *B*, then $H(A,B) = d$. Thus, even if the shapes represented by the two remaining data sets are almost identical, the Hausdorff distance will not reflect this fact.

We can avoid this problem by using the *partial* Hausdorff distance (Huttenlocher and Rucklidge 1992):

$$h_k(A,B) = \underset{a \in A}{kth} \min_{b \in B} \|a - b\| \tag{3}$$

---

[1] A Hölder *norm* L_p is a generalization of the Euclidean distance between two points in $\Re^n$, and is defined as $L_p = \|\bar{r}\|_p = \left(\sum_{i=1}^{n} |r_i|^p \right)^{\frac{1}{p}}$ for some *n*-dimensional vector $\bar{r}$ (e.g., Golub and van Loan 1983). For two dimensions (i.e., $\Re^2$) then, the Euclidean distance is given by $L_2 = \|\bar{r}\|_2 = \sqrt{r_x^2 + r_y^2}$.

where *k*th denotes the *k*-th ranked value. This measure does not obey the metric properties we require. However, it does partition *A* into two subsets: those points which are close to the points of *B* (that is, within distance $h_k(A,B)$, and those which are the outliers. Both subsets obey the metric properties.

This can be very useful. By choosing some value *k*, we can obtain a measure of the degree of dissimilarity between the two subsets $A_k = \{a_1,\ldots,a_{p-k}\}$ and $B_k = \{b_1,\ldots,b_{q-k}\}$, and also identify the outliers and their degree of dissimilarity.

A further advantage of the Hausdorff distance metric is its extreme simplicity. The time complexity[2] for a trivial implementation is $O(pq)$, and Alt et al. (1991) have shown that this can be improved to $O((p+q)\log_2(p+q))$. However, given the relatively small data sets associated with most photometric distributions (on the order of 200 to 400 points), it is likely that the processor time will be dominated by input and parsing of the ASCII data files. Thus, the trivial (i.e., easily programmed) implementation should be sufficient.

6. Geometric Transformations

Shape analysis techniques should be invariant with respect to translation, rotation, and scaling of the object in an image. That is, shape analysis techniques should measure shape alone; they should not be affected by any transformation of the image that preserves the geometric properties of the object.

Translation invariance: moving one object from one location in the image to another location should not affect the analysis outcome once the two objects have been aligned (where "aligned" means that the Hausdorff distance metric $H(A,B)$ is minimal). In our case, there is no translation – the photometric solid is anchored at the origin.

Rotation invariance: rotating the object about some point in the image plane should not affect the analysis outcome after alignment. This is clearly desirable – we may for example choose to compare the beam patterns of two theatre spotlights by rotating one of their photometric distributions ten degrees about a horizontal axis.

Scaling invariance: changing the size of an object should not affect the analysis outcome after alignment. This is logical in that the geometric shape of the photometric distribution does not change with scaling. (As an aside, the European CIE 102 (CIE 1993) and EULUMDAT photometric data file formats explicitly scale photometric distributions by expressing luminous intensity values in units of candela per 1,000 lamp lumens. This contrasts with the North American LM-63 format (IESNA 1995), which expresses intensity in units of the rated test lamp lumens.)

As noted by Rucklidge (1994), the Hausdorff distance metric is invariant under translation, rotation, and scaling after alignment

7. The Photometric Solid

Most shape analysis techniques are designed for analyzing two-dimensional images, and so we have so far considered the comparison of photometric distributions based on single vertical planes. However, it is evident that the photometric distribution is a continuous function in three dimensions, as shown by the photometric solid (Figure 2). It therefore makes sense to compare photometric distributions based on these solids.

---

[2] The *time complexity* $O(f(n))$ of an algorithm means that the time needed to perform its calculations is proportional to the value of the function $f(n)$, where *n* is the size of the data set. Thus, the Hausdorff distance metric calculation with a time complexity of $O(pq)$ for point sets $A = \{a_1,\ldots,a_p\}$ and $B = \{b_1,\ldots,b_q\}$ has an execution time proportional to *pq*.

From Equations 1 and 2, it is evident that the Hausdorff distance metric is applicable in *n*-dimensional space. We can therefore apply it to the complete set of luminous intensity values (translated from spherical to Cartesian coordinates) for each photometric distribution.

There is some danger here. Our comparison should produce a distribution ranking that appears intuitively correct to someone viewing the photometric distributions as two-dimensional plots (e.g., Figure 1). It is possible that two distributions with similar shapes in the zero-degree vertical plane will have an unexpectedly large Hausdorff distance because the distributions in the other planes differ significantly. With this in mind, it will be prudent to provide the user with a choice of two rankings: the photometric solid and a selected vertical plane.

We must also recognize that two distributions with identical shapes but with different sizes will not be recognized as being similar by the Hausdorff distance metric. Whether this is important will depend on the application. If it is, then the photometric distributions should be "normalized" by dividing each intensity value by the calculated total emitted luminous flux of the light source (IESNA 1982).

Finally, we should remember that photometric distributions for most architectural luminaires are sparsely sampled about the vertical axis. (Typical values are 22.5-degree increments in North America and 15.0-degree increments in Europe.) Luminaires that exhibit strong asymmetries about the vertical axis may have measured photometric distributions whose Hausdorff distance is not representative of the dissimilarity between their true photometric solids.

8. Implementation Issues

If we consider photometric distributions based on physical measurements only, we will likely find that the distribution outlines are relatively smooth in each vertical plane. However, the same may not be true of synthesized photometric distributions produced by some luminaire design programs.

The problem is that these programs rely on stochastic ray casting to predict the luminous intensity distributions of architectural luminaires and other light sources. This is a compute-intensive process, and users are often tempted to terminate the process before a sufficient number of rays have been cast. The resultant distributions then exhibit significant stochastic sampling errors, particularly towards zenith and nadir where the density of randomly cast rays decreases. (The solid angle density remains constant, but the density per constant angular increment in each vertical plane decreases towards the poles.)

Given an undersampled synthetic distribution as an example, it is less likely that an appropriate ranking of physical photometric distributions will be achieved. To alleviate this problem, the user should be given the opportunity to interactively smooth the synthetic distribution data.

Press et al. (1992) suggest filtering data in the frequency domain after using a fast Fourier transform (FFT). This is appropriate for smoothing photometric distribution data, as it can be represented by a continuous periodic function $f(r,\theta,\phi)$ in spherical coordinates. It is only necessary to interpolate the data across $2^m \times 2^n$ points before performing a two-dimensional FFT, and interpolate it again after performing the inverse FFT to restore the original number of data points.

Smoothing in the frequency domain requires multiplying the magnitude of each frequency coefficient by a scaling factor. To simplify the user interface, a smoothing parameter *s* could be applied according to:

$$L(\omega) = \begin{cases} 1 & ,\omega \le s \\ 0 & ,\omega > s \end{cases} \tag{4}$$

where $L(\omega)$ represents the transfer function of an ideal low-pass filter.

Finally, the user may wish to selectively emphasize certain angular regions of a photometric distribution for comparison purposes. For example, it may be important to determine whether the angular extent of a theatrical spotlight beam exceeds a specific range. If both data sets have the same number of points (or if one is interpolated to achieve this), a simple but effective approach is to scale corresponding values in both sets according to:

$$\begin{aligned} a'_{\theta,\phi} &= ma_{\theta,\phi} - (m-1)\left(\frac{a_{\theta,\phi} + b_{\theta,\phi}}{2}\right) \\ b'_{\theta,\phi} &= mb_{\theta,\phi} - (m-1)\left(\frac{a_{\theta,\phi} + b_{\theta,\phi}}{2}\right) \end{aligned} \tag{5}$$

where $m \geq 0$ is the scaling factor.

The smoothing and scaling parameters are necessarily heuristics that must be individually determined for each application. Fortunately, their operation is intuitive and the resultant photometric distributions can be viewed graphically in real time.

9. Experimental Results

A computer program was written to examine the performance of the Hausdorff distance metric. The criteria were necessarily subjective – the metric should rank distributions in a manner similar to that of an experienced illumination engineer. Still, there should be general agreement on the ranking, especially when a large number of comparisons are performed.

The program required approximately 0.5 seconds to calculate the metric for each IESNA LM-63 or EULUMDAT data file on a Pentium 450 MHz desktop computer. This included the time required to read and parse each file. Thus, the metric is computationally efficient and suitable for interactive use.

Figure 3 illustrates the results of one experiment wherein the template distribution shown in Figure 1 (an indirect linear fluorescent luminaire) was compared against sixty-four different distributions from the luminaire product line. These included direct, indirect, direct-indirect and asymmetric distributions. The distributions were not normalized prior to comparison. Subjectively, the comparison distributions appear to be similar to the template, and the ranking is similar to what lighting designers would likely choose.

Figure 4 illustrates the results of another experiment with normalized distributions, and with a direct-indirect linear fluorescent luminaire providing the template distribution. The ranking by shape is reasonably intuitive, but the range of emitted flux values is beyond that which most lighting designers would consider as representing similar luminaires. (In practice, the program allows the user to specify a range of luminous flux values to consider when performing comparisons.)

Figures 3 and 4 further illustrate that the Hausdorff distance metric values are dependent on the distribution intensities. If the distributions are scaled by some factor, then their calculated *HDM* values will be scaled by the same factor. This underscores an important point: no particular significance should be assigned to any given metric value. The Hausdorff distance metric is useful only for ranking purposes.

While our assessment of whether the rankings shown in Figures 3 and 4 are appropriate is necessarily subjective, it is evident that the seven distributions are similar to the template in both cases. While different rankings can be obtained by fine tuning the comparison criteria, the approach clearly works.

10. Conclusions

Of the many pattern classification algorithms that have been proposed in the literature, the Hausdorff distance metric is one of the few that are suited for comparing photometric

distributions. It is easy to understand, computationally efficient, and adaptable to the varying requirements of illumination engineering and lighting design.

At the same time, the Hausdorff distance metric does not provide a computer program with the intelligence of an experienced illumination engineer or lighting specifier. There are undoubtedly pathological cases where it will fail to provide reasonable rankings. Rather, it provides a useful computer tool whose output may require some interpretation and judgment.

Illumination engineers and lighting specifiers are often faced with the task of searching dozens of manufacturers' catalogs for light sources with similar photometric distributions. If the manufacturers' photometric data files are available, the Hausdorff distance metric can turn a tedious and time-consuming manual task into a simple computer chore.

11. Acknowledgements

Thanks to Dr. Jack Snoeyink of the University of British Columbia for providing the academic incentive to research and prepare this paper, and for reminding me that the ultimate goal of writing is to communicate.

12. References

Alt, H., B. Behrends, and J. Blomer. 1991. "Approximate Matching of Polygonal Shapes," Proc. Seventh ACM Symposium on Computational Geometry, pp. 186-193.

Alt, H., and M. Godau. 1992. "Measuring the Resemblance of Polygonal Curves," Proc. Eighth ACM Symposium on Computational Geometry, pp. 102-109.

Arkin, E. M., L. P. Chew, D. P. Huttenlocher, K. Kedem, and J. S. B. Mitchell. 1986. "An Efficiently Computable Metric for Comparing Polygonal Shapes," IEEE Transactions on Pattern Analysis and Machine Intelligence PAMI-13(3):209-216 (March).

Belkasim, S. O., M. Shridhar, and M. Ahmadi. 1991. "Pattern Recognition with Moment Invariants: A Comparative Study and New Results," Pattern Recognition 24(12):1117-1138.

Blum, H. 1977. "A Transformation for Extracting New Descriptors of Shape," in Models of the Perception of Speech and Visual Forms, W. Whaten-Dunn, Ed., pp. 362-380. Cambridge, MA: MIT Press.

Chang, C. C., S. M. Hwang, and D. J. Buehrer. 1991. "A Shape Recognition Scheme Based on Relative Distances of Feature Points From the Centroid," Pattern Recognition 24(11):1053-1063.

Chuang, G. C. H., and C. C. J. Kuo. 1996. "Wavelet Descriptor of Planar Curves: Theory and Applications," IEEE Transactions on Image Processing 5(1):56-70 (January).

CIE Technical Committee 4-16. 1993. Recommended File Format for electronic Transfer of Luminaire Photometric Data, Technical Report CIE 102-1993. Vienna, Austria: Commission Internationale de l'Eclairage (International Commission on Illumination).

Cohen, F. S., Z. Huang, and Z. Yang. 1995. "Invariant Matching and Identification of Curves Using B-Splines Curve Representation," IEEE Transactions on Image Processing 4(1):1-10.

Cortelazzo, G., G. A. Mian, G. Vezzi, and P. Zamperoni. 1994. "Trademark Shapes Description by String-matching Techniques," Pattern Recognition 27(8):1005-1018.

Das, M., M. J. Paulik, and N. K. Loh. 1990. "A Bivariate Autoregressive Modeling Technique for Analysis and Classification of Polygonal Shapes," IEEE Transactions on Pattern Analysis and Machine Intelligence PAMI-12:97-103.

Dubois, S., and F. Glanz. 1986. "An Autoregressive Model Approach to Two-Dimensional Shape Classification," IEEE Transactions on Pattern Analysis and Machine Intelligence PAMI-8(1):55-66 (January).

Eom, K. B. 1998. “Shape Recognition Using Spectral Features,” Pattern Recognition Letters 19:189-195.

Godau, M. 1991. “A Natural Metric for Curves – Computing the Distance for Polygonal Chains and Approximation Algorithms,” Lecture Notes in Computer Science 480: STACS 91 (Eighth Annual Symposium on Theoretical Aspects of Computer Science). C. Choffrut and M. Jantzen, Eds. New York, NY: Springer-Verlag, pp. 127-136.

Golub, G. H., and C. F. van Loan. 1983. Matrix Computations. Baltimore, MD: John Hopkins University Press.

Goshtasby, A. 1985. “Description and Discrimination of Planar Shapes Using Shape Matrices,” IEEE Transactions on Pattern Analysis and Machine Intelligence PAMI-7:738-743.

Gunsel, B., and A. M. Tekalp. 1998. “Shape Similarity Matching for Query-by-Example,” Pattern Recognition 31(7):931-944 (July).

He, Y., and A. Kundu. 1991. “2-D Shape Classification Using Hidden Markov Model,” IEEE Transactions on Pattern Analysis and Machine Intelligence PAMI-13(11):1172-1184 (November).

Huttenlocher, D. P., G. A. Klanderman, and W. J. Rucklidge. 1993. “Comparing Images using the Hausdorff Distance,” IEEE Transactions on Pattern Analysis and Machine Intelligence PAMI-15(9):850-863 (September).

Huttenlocher, D. P., and W. J. Rucklidge. 1993. A Multiresolution Technique for Comparing Images Using the Hausdorff Distance. Department of Computer Science Technical Report TR92-1321. Ithaca, NY: Cornell University.

IESNA Calculation Procedures Committee. 1982. Calculating Coefficients of Utilization, Wall Exitance Coefficients, and Ceiling Cavity Exitance Coefficients, IESNA LM-57-82. New York, NY: Illuminating Engineering Society of North America.

IESNA Computer Committee. 1995. IESNA Standard File Format for Electronic Transfer of Photometric Data, IESNA LM-63-95. New York, NY: Illuminating Engineering Society of North America.

Jacobs, C. E., A. Finkelstein, and D. H. Salesin. 1995. “Fast Multiresolution Image Querying,” Proceedings of SIGGRAPH ’95, pp. 277-286.

Kashyap, R., and R. Chellappa. 1981. “Stochastic Models for Closed Boundary Analysis: Representation and Reconstruction,” IEEE Transactions on Information Theory IT-27(5):627-637 (September).

Levin, R. E. 1984. “Interpolation of Intensity Distributions,” Journal of the Illuminating Engineering Society 13(10):27-35 (October).

Lin, Y., J. Dou, and H. Wang. 1992. “Contour Shape Description Based on an Arch Height Function,” Pattern Recognition 25(1):17-23.

Loncaric, S. 1998. “A Survey of Shape Analysis Techniques,” Pattern Recognition 31(8):983-1001 (August).

Mallet, Y., D. Coomans, J. Kautsky, and O. D. Vel. 1997. “Classification Using Adaptive Wavelets for Feature Extraction,” IEEE Transactions on Pattern Analysis and Machine Intelligence PAMI-19(10):1058-1066 (October).

Neil, G., and K. M. Curtis. 1997. “Shape Recognition Using Fractal Geometry,” Pattern Recognition 30(12):1957-1969 (December).

Parui, S., E. Sarma, and D. Majumder. 1986. “How to Discriminate Shapes Using the Shape Vector,” Pattern Recognition Letters 4:201-204.

Pavlidis, T., and F. Ali. 1979. “A Hierarchical Syntactic Shape Analyzer,” IEEE Transactions on Pattern Recognition and Machine Intelligence PAMI-1(1):2-9 (January).

Persoon, E., and K. S. Fu. 1986. “Shape Discrimination Using Fourier Descriptors,” IEEE Transactions on Pattern Analysis and Machine Intelligence PAMI-8(3):388-397 (May).

Press, W. H., B. P. Flannery, S. A. Teukolsky, and W. T. Vetterling. 1992. Numerical Recipes in C: The Art of Scientific Computing. Cambridge, MA: Cambridge University Press.

Rucklidge, W. J. 1994. Lower Bounds for the Complexity of the Hausdorff Distance. Department of Computer Science Technical Report TR94-1441. Ithaca, NY: Cornell University.

Smith, S. P., and A. K. Jain. 1982. “Chord Distribution for Shape Matching,” Computer Graphics and Image Processing 20:259-271.

Sze, T. W., and Y. H. Yang. 1981. “A Simple Contour Matching Algorithm,” IEEE Transactions on Pattern Analysis and Machine Intelligence PAMI-3(6):676-678 (November).

Teague, M. R. 1980. “Image Analysis via the General Theory of Moments,” Journal of the Optical Society of America 70:920-930.

Wang, S., P. Chen, and W. Lin. 1994. “Invariant Pattern Recognition by Moment Fourier Descriptor,” Pattern Recognition 27(12):1735-1742.

Yamauti, Z. 1932. “Theory of Field of Illumination,” Researches of the Electrotechnical Laboratory, No. 339 (October). Tokyo, Japan: Ministry of Communications.

CATALOG NO.:			8216T01PN
Lamp Type:	FO32T8 (EO)	Description:	
No. of Lamps:	1		
Rated Lamp Lumens:	2900		
Ballast Input Watts:	37.9	Optical Efficiency:	84.8%
CIE-IES Classification:	#REF!	Lab Report No.:	2100546;

CANDELA DISTRIBUTION

	0	22.5	45	67.5	90	Flux Lumens
0	296	296	296	296	296	
5	296	295	297	297	300	29
15	278	286	307	332	358	89
25	240	266	345	401	425	156
35	173	237	325	369	365	183
45	65	117	165	172	144	108
55	9	15	21	25	33	22
65	1	4	4	9	12	6
75	0	0	0	2	1	1
85	0	0	0	0	0	0
90	0	0	0	0	0	
95	9	89	51	58	42	71
105	53	188	338	371	335	279
115	109	225	380	506	554	356
125	168	237	413	503	536	337
135	223	268	390	510	551	299
145	269	300	355	429	473	230
155	306	324	355	381	396	164
165	331	340	352	364	370	100
175	344	345	347	349	350	34
180	346	346	346	346	346	

POLAR CANDELA PLOT

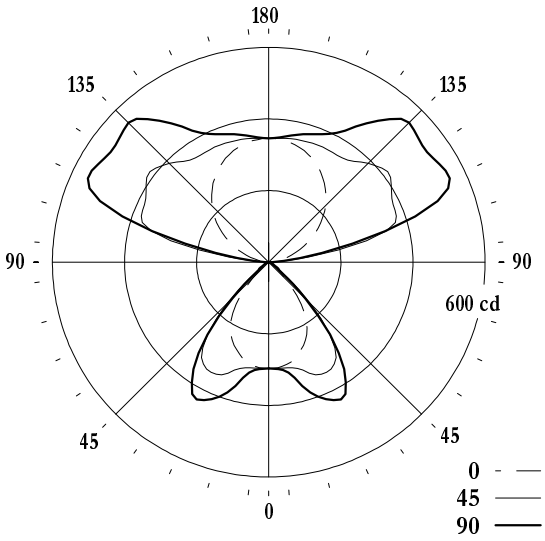

02/11/97

COEFFICIENTS OF UTILIZATION (%)

Pc---	80				70			50			0
Pw---	70	50	30	10	70	50	30	50	30	10	0
RCR											
0	85	85	85	85	76	76	76	58	58	58	20
1	78	75	72	70	70	67	65	52	50	49	18
2	72	66	62	58	64	59	56	46	44	42	16
3	66	59	53	49	59	53	48	41	38	36	15
4	61	52	46	42	54	47	42	37	34	31	13
5	56	47	41	36	50	42	37	33	30	27	12
6	51	42	36	31	46	38	33	30	26	24	11
7	48	38	32	28	42	34	29	27	24	21	10
8	44	34	28	24	39	31	26	25	21	19	9
9	41	31	26	22	37	28	23	23	19	17	8
10	38	29	23	19	34	26	21	21	17	15	7

*Based on a floor reflectance of 0.2

Figure 1 – Typical photometric distribution report

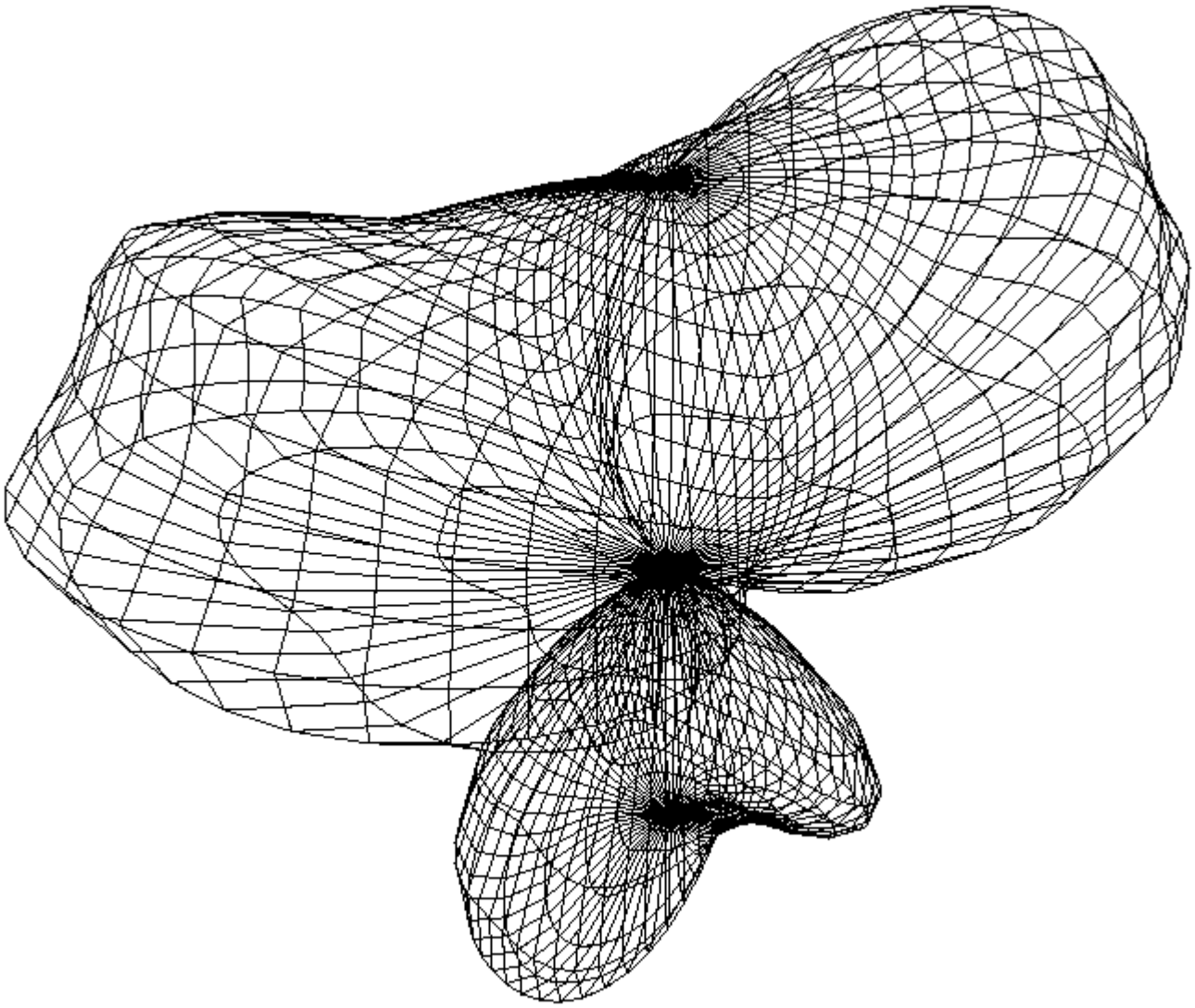

Figure 2 – Equivalent “photometric solid” of Figure 1

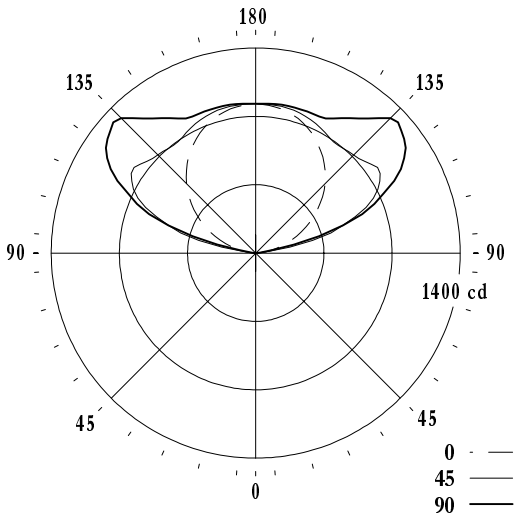

8213F2EN.IES (template)
Emitted flux = 4293 lm (1.00)

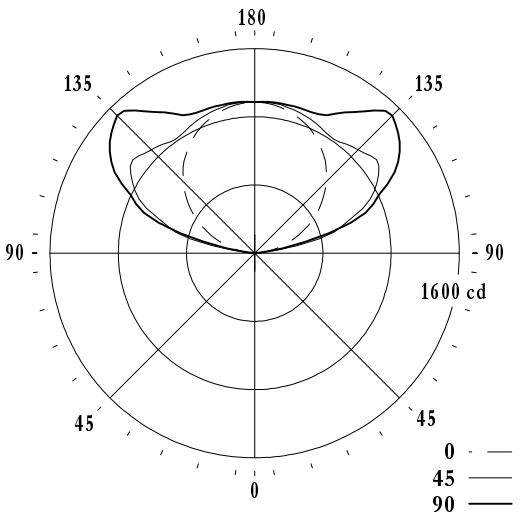

8213B1EN.IES (HDM = 123.0)
Emitted flux = 5051 lm (1.17)

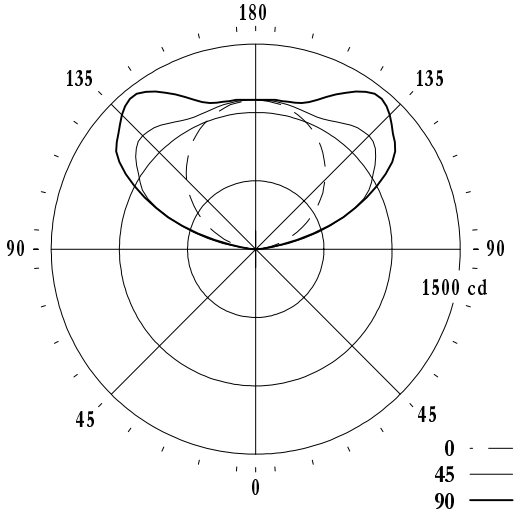

8213T2EN.IES (HDM = 178.6)
Emitted flux = 4639 lm (1.08)

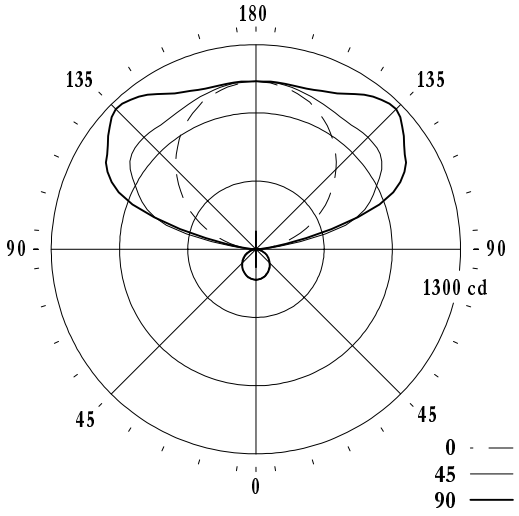

8215B1LN.IES (HDM = 227.7)
Emitted flux = 4957 lm (1.15)

Figure 3 – Hausdorff distance metric comparsion

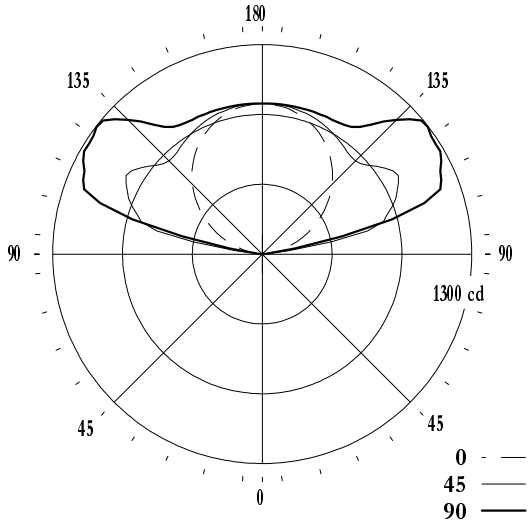

8213H1EN.IES (HDM = 235.1)
Emitted flux = 4354 lm (1.01)

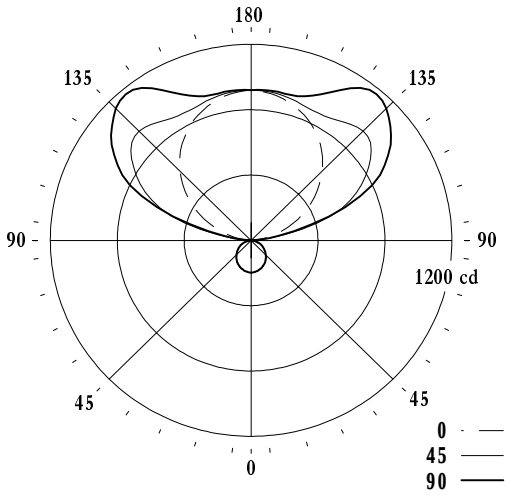

8215T2EN.IES (HDM = 328.9)
Emitted flux = 4334 lm (1.00)

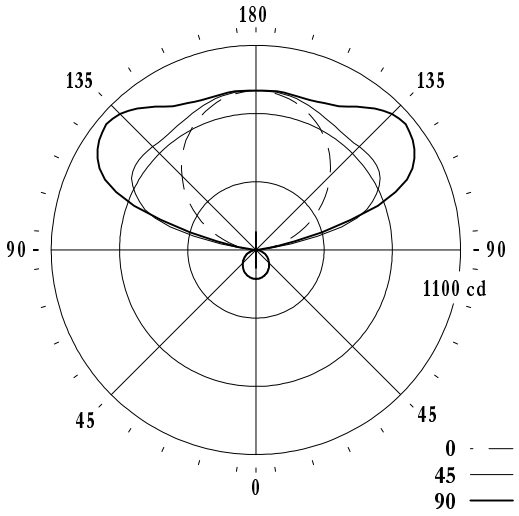

8215F2LN.IES (HDM = 410.4)
Emitted flux = 3989 lm (0.92)

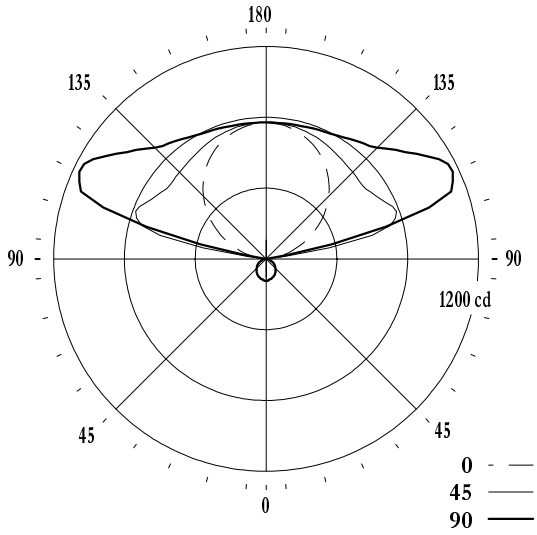

8215H1LN.IES (HDM = 461.3)
Emitted flux = 3903 lm (0.90)

Figure 3 continued – Hausdorff distance metric comparsion

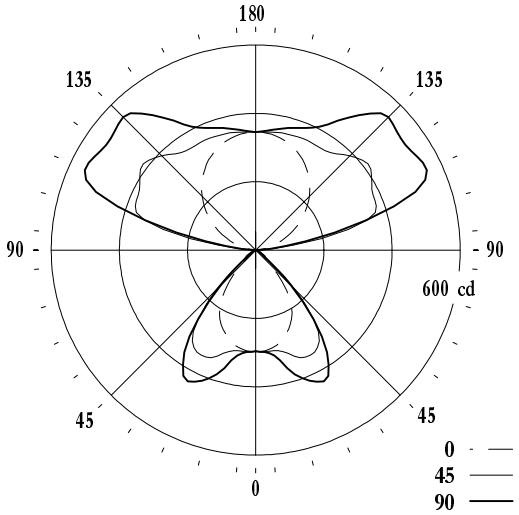

8216T1PN.IES (template)
Emitted flux = 2458 lm (1.00)

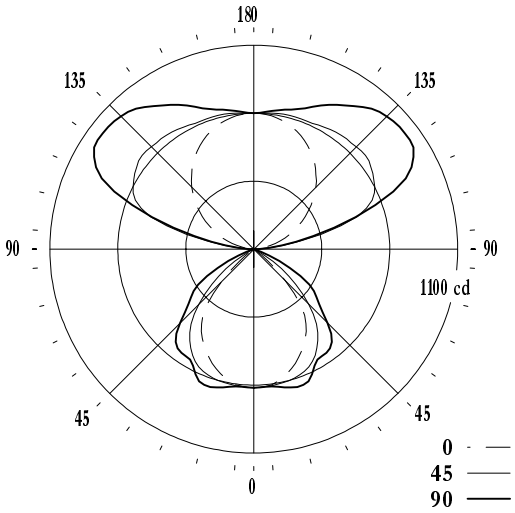

8226T2PN.IES (HDM = 0.03440)
Emitted flux = 5073 (2.06)

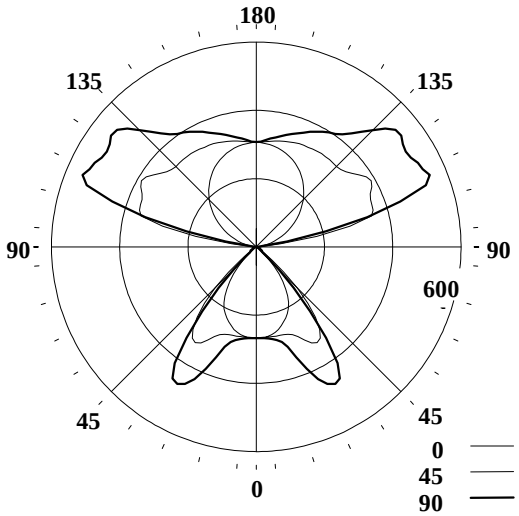

8216F1PN.IES (HDM = 0.0347)
Emitted flux = 2251 m (0.52)

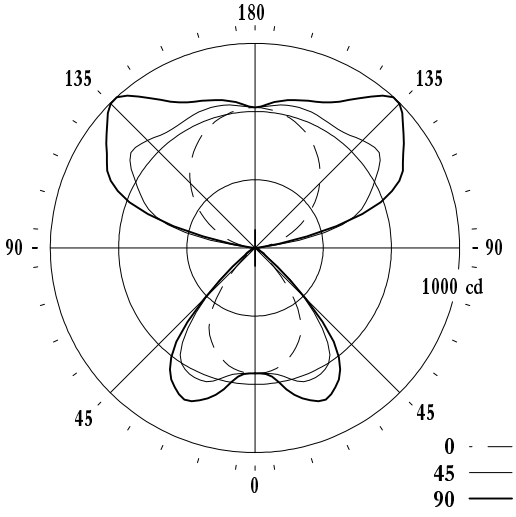

8216F2PN.IES (HDM = 0.0414)
Emitted flux = 4447 lm (1.80)

Figure 4 – Hausdorff distance metric comparsion (normalized)

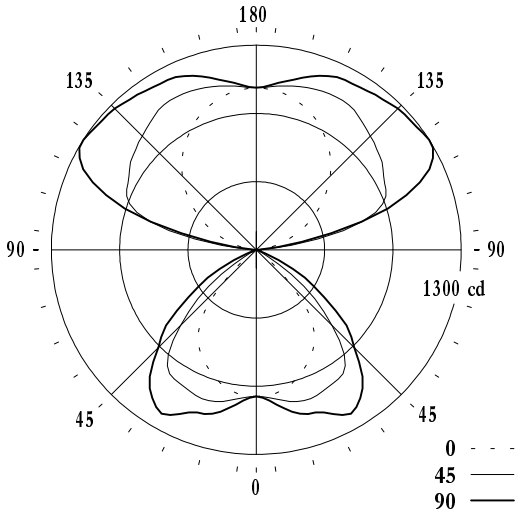

8226F3PN.IES (HDM = 0.0437)
Emitted flux = 6985 lm (2.84)

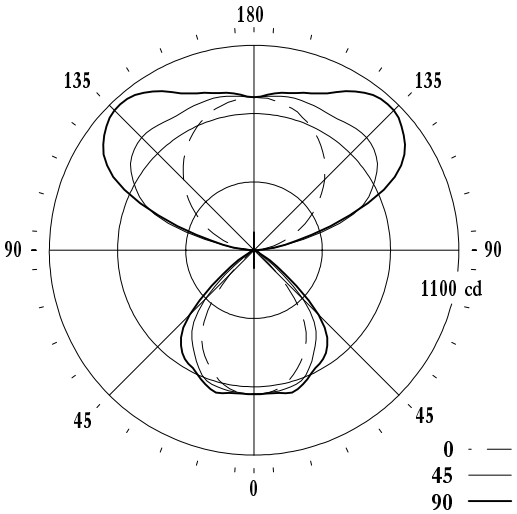

8216T2PN.IES (HDM = 0.0449)
Emitted flux = 4955 lm (2.01)

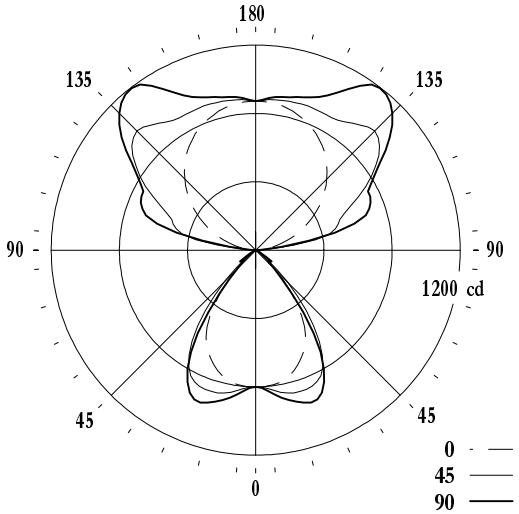

8216B1PN.IES (HDM = 0.0617)
Emitted flux = 5200 lm (2.11)

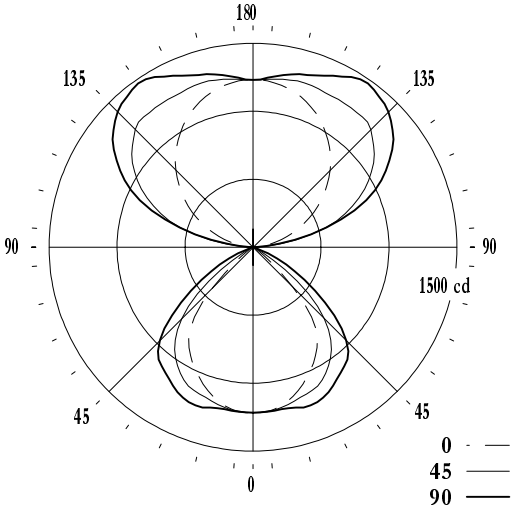

8226T3PN.IES (HDM = 0.0697)
Emitted flux = 7623 lm (3.10)

Figure 4 continued – Hausdorff distance metric comparsion (normalized)